The pyruvate kinase activator mitapivat reduces hemolysis and improves anemia in a β-thalassemia mouse model

Matte et al.

Supplemental data

Methods

Drugs and chemicals

NaCl, Na_3VO_4, bicine, Tris, Tween 20, choline, $MgCl_2$, glycine, MOPS, hydrocortisone, benzamidine, β-mercaptoethanol, SDS, NaF, EDTA, May-Grünwald stain, Giemsa stain, erythropoietin, BSA, glycerol, Luminata Forte and Luminata Classico HRP solutions, and dithiothreitol were obtained from Merck KGaA; protease inhibitor cocktail tablets were from Roche; Triton X-100, prestained Protein Ladder, and TEMED were from GE Healthcare; 40% acrylamide/bisacrylamide solution, 37.5:1, was from Bio-Rad; Dulbecco's PBS was from Lonza; Iscove's Modified Dulbecco's Medium, α-MEM was from Gibco; penicillin-streptomycin, L-glutamine, and fetal calf serum were from Thermo Fisher Scientific; amphotericin was from EuroClone; MethoCult M3234 was from STEMCELL Technologies.

Mouse studies

Where mitapivat was administered by addition to the mouse diet, 1200 ppm w/w was added to the Mod LabDiet 5P00 standard rodent diet, which corresponds to the oral 50 mg/kg twice a day (BID) dosage of mitapivat, as determined in preliminary experiments. Based on the calculation of human equivalent dose by body surface area according to Reagan-Shaw et al. (1), the mouse mitapivat dose in the current study is close to the higher dose administered in a human study (mouse dose in current study = 50 mg/kg BID; Human dose in mitapivat clinical trial (NCT03692052) 100 mg BID). The iron content of both control- and mitapivat-enriched diets was 379 ppm, corresponding to the mouse standard diet.

Red cell survival

Red cells from WT and $Hbb^{th3/+}$ mice treated with or without mitapivat were labeled with CFSE (10μM; Molecular Probes, Invitrogen) in PBS 0.5% BSA for 20 minutes at 37°C. After quenching with PBS 1% FBS, red cells were washed 3 times with sterile

PBS and resuspended at approximately 2 × 10^9 cells in 250 µL of sterile PBS. Mice were injected intravenously with the CFSE-labeled red cells, the kinetics of disappearance of labeled cells from circulation was measured by flow-cytometry using a FACS Canto flow cytometer (BD Biosciences) and data were analyzed by Flow Jo software (Tree Star).

Red cell western blot analysis

Red cells were analyzed either in unfractionated form or after separation on a discontinuous Percoll density gradient that yielded fraction 1 (F1) corresponding to a density of N1.074 (containing reticulocyte enriched red cell fraction) and fraction 2 (F2) corresponding to a density of N1.092 (containing the densest and oldest red cells) as previously described (2).

Flow cytometric analysis of mouse erythroid precursors and molecular analysis of sorted erythroid cells

The following antibodies were used: anti-CD16/CD32 blocking agent (Affimetrix Bioscence clone 93), anti–CD44-FITC (eBioscence clone IM7), anti–CD71-PE (Macs clone Ac-102), anti–Ter119-APC (# 17-5921, eBioscience, ThermoFisher Scientific), CD45 APC-eFluor 780 (clone 30F-11, eBioscience, ThermoFisher Scientific), GR1 APC-Cy7 (clone RB6-8C5, eBioscience) and CD11b APC-Cy7 (clone M1/70, eBioscience). Dead cells were detected using 7-aminoactinomycin D (Becton Dickinson), added 2 minutes before analysis. Flow cytometric analysis of the mitochondria was carried out using the MitoTracker Deep Red probe (Thermo Fisher Scientific), following the manufacturer instructions. Briefly, 500,000 cells from bone marrow were incubated with the following antibodies: anti–CD44-FITC, CD71-PE, Ter119-V450 (# 48-5921, eBioscience) for 30 minutes at 4°C. After 2 washes with PBS BSA 1%, cells were incubated in PBS BSA 1% with MitoTracker Deep Red probe (500 nM) for 30 minutes at 37°C. After 2 washes with PBS BSA 1%, cells were immediately analyzed. Flow cytometric analysis was carried out with the FACSCanto II flow cytometer (Becton Dickinson). The biparametric scatter plots were analyzed with FlowJo software version 10 (Tree Star). Based on the CD44-Ter119 gating strategy, cells were sorted using the BD FACS Aria III cell sorter (Becton Dickinson).

Quantitative real-time (qRT) PCR on sorted erythroblasts

mRNA was isolated and reverse transcribed into high-purity cDNA using μMACS One-step cDNA Kit according to the manufacturer's instructions (Miltenyi Biotec). We started from 400,000 sorted polychromatic and orthochromatic erythroblasts from bone marrow of the different mouse strains. One-fiftieth of the reactions were added to appropriate wells of the PCR plates. qRT-PCR was performed with SYBR Green PCR Master Mix (Applied Biosystems) using Applied Biosystems Model 7900HT Sequence Detection System. Detailed primer sequences are available in Supplemental Table 1. All PCR reactions were performed in triplicate. Relative gene expression was calculated using the $2^{-\Delta Ct}$ method, in which Ct indicates cycle threshold, the cycle number where the fluorescent signal reaches the detection threshold. ΔCt was computed by calculating the difference of the average Ct between the test gene and the internal control gene, *Gapdh*.

Evaluation of mitochondrial complex I in sorted erythroblasts

Twenty-three micrograms of whole-cell lysates were prepared with CHAPS buffer (1% CHAPS, 100 mM KCl, 50 mM HEPES pH 7.5, 1 mM EGTA; supplemented with protease/phosphatase inhibitors, Sigma-Aldrich), were equally loaded (bicinchoninic acid protein assay), resolved using SDS PAGE, precast 4%–12% gels (Novex, Life Technologies), and transferred onto PVDF membranes (Amersham Hybond 0.45 μm, GE Healthcare). Membranes were blocked with 2% BSA, tris buffered saline 0.1% tween, and then incubated with primary antibody for NDUFB8 (Molecular Probes) and β-actin (SIGMA) followed by 1:10,000 HRP-conjugated secondary antibodies (Santa Cruz Biotechnology). Visualization of antibody protein complexes was achieved by enhanced chemiluminescence (LiteAblot turbo, EuroClone) and the ChemiDoc XRS+ System (Bio-Rad). Densitometry was performed with the Gel-Pro Analyzer software (3).

Measurement of ATP in sorted erythroblasts

ATP was measured in sorted erythroblasts using the CellTiter-Glo® Luminescent Cell Viability Assay (Promega) following the manufacturer instructions; 1.5 million sorted erythroblasts were used. The luminescent signal was recorded using the Victor

Multilabel plate reader (PerkinElmer) and cell ATP concentration was determined by plotting values onto a standard curve, ranging from 0.1 μM to 24 μM of ATP.

Liver and C-duodenum molecular analysis: RNA isolation, cDNA preparation, and qRT-PCR

Total RNA was extracted from mouse tissues using TRIzol reagent (Life Technologies). Synthesis of cDNA from total RNA (2 μg) was performed using SuperScript II First Strand kits (Life Technologies). qRT-PCR was performed using the SYBR Green method as described above.

Liver and C-duodenum western blot analysis

Frozen livers from WT and $Hbb^{th3/+}$ mice were homogenized and lysed with ice cold lysis buffer (150 mM NaCl, 25 mM bicine, 0.1% SDS, 2% Triton X-100, 1 mM EDTA, protease inhibitor cocktail tablets, 1 mM Na_3VO_4 final concentration) followed by centrifugation for 30 minutes at 4°C at 12,000*g*. Proteins were quantified then separated by monodimensional SDS-PAGE. Proteins were transferred to nitrocellulose membranes for western blot analysis with specific antibodies: STAT3 (clone C-20, Santa Cruz Biotechnology); Phospho- Ser536 NF-κb p65 (pNF-κb p65, # 3031, Cell Signaling Technology), NF-κb p65 (clone C22B4, Cell Signaling Technology), HIF2α (clone 190b; Santa Cruz Biotechnology), Phospho-Thr202/Tyr204 p44/42 PERK (clone D13.14.4E; Cell Signaling Technology), and p44/42 ERK1/2 (clone 137F5, Cell Signaling Technology); Phospho-Tyr705 pSTAT3 (clone EP2147Y; AbCam); STAT3 (clone C-20, Santa Cruz Biotechnology), Phospho Ser40 NRF2 (pNRF2, clone EP1809Y, AbCam), and NRF2 (clone EP1809Y, Abcam); anti-PKR and anti-PKM2 were kindly gifted by Agios. Anti-GAPDH (clone D6, Santa Cruz Biotechnology) was used as loading control. Secondary donkey antirabbit IgG and antimouse IgG HRP conjugates were from GE Healthcare Life Sciences, secondary donkey antigoat HRP conjugate was from Santa Cruz Biotechnology. Blots were developed using the Luminata Forte Chemiluminescent HRP Substrate from Merck KGaA, and images were acquired using Image Quant Las Mini 4000 Digital Imaging System (GE Healthcare Life Sciences). To analyze PKM2 dimers and tetramers, C-duodenal proteins were solubilized in the presence of the cross-linker disuccinimidyl suberate (Thermo Fisher Scientific), following the manufacturer's instructions (4). Liver oxidized proteins were monitored using OxyBlot

Protein Oxidation Detection Kit (EMD Millipore) as previously reported (5), briefly, carbonylated proteins were detected by treating with 2,4-dinitrophenylhydrazine (DNPH) and blotted with anti- dinitrophenyl antibody. Densitometric analyses were performed using the ImageQuant TL software (GE Healthcare Life Sciences).

Liver and spleen iron content

Spleen and liver samples were dried at 65°C overnight and weighed. Then, 10 mg of dry tissue were digested in 1 mL of acid solution (3 M HCl, 0.6 M trichloroacetic acid) at 65°C for 16 hours. Next, 20 µL of the acid extract were analyzed using 1 mL of chromogen solution (0.1% bathophenanthroline sulfate, 1% idrossilammine, and 10% sodium acetate pH 6.5), evaluating the absorbance at 535 nm. A standard curve was generated using an acid solution containing increasing amounts of iron sulfate.

Ferroportin (FPN1) immunohistochemistry

Five-micrometer thick duodenum sections were deparaffinized, treated in citrate buffer (1 mM, pH 6.0) for 15 minutes, washed, and incubated with 3% H_2O_2 for 10 minutes. Slides were blocked in 1% BSA for 1 hour at room temperature, followed by overnight incubation with rabbit anti-FPN1 antibody (MTP11-A, Alpha Diagnostics), then with biotinylated goat antirabbit antibody (Vector Laboratories) for 30 minutes at room temperature. The stain was visualized with 3,3'-diaminobenzidine (Sigma-Aldrich).

ERFE assay

Mouse ERFE monoclonal antibodies and recombinant mouse ERFE standard were donated by Silarus Therapeutics. Yellow DELFIA 96-well high-binding plates (PerkinElmer #AAAND-0001) were coated overnight at 4°C with 100 µL/well of 1.0 µg/mL capture antibody in Dulbecco's PBS buffer (GE Healthcare #SH30028.03). Plates were washed with 200 µL DELFIA wash buffer per well (PerkinElmer #1244-114) 3 times, then blocked for 1 hour with 200 µL/well 1% BSA in Dulbecco's PBS buffer (PerkinElmer #CR84-100). Samples and standards diluted in DELFIA assay buffer (PerkinElmer #1244-106) were incubated for 2 hours at room temperature on a plate shaker at 300 rpm. Plates were washed 3 times and incubated for 1 hour with 100 µL/well of 1.0 µg/mL biotinylated detection antibody in DELFIA assay buffer,

washed 3 times, and then incubated for 20 minutes (with black cover) with Europium-Streptavidin (PerkinElmer #1244-360). Plates were developed with 200 µL/well DELFIA enhancement solution (PerkinElmer #1244-104) in the dark at room temperature for 5 minutes, then the plates were read with CLARIOstar time-resolved fluorescence filter/flash lamp (BMG LABTECH).

Studies of in vitro human erythropoiesis

Light-density mononuclear cells were obtained by centrifugation on Lymphoprep (STEMCELL Technologies) density gradient, as previously described (6, 7). The $CD34^+$ cells were positively selected by anti-CD34-tagged magnetic beads (MiniMACS columns; Miltenyi Biotec) according to the manufacturer's protocol. The recovery was more than 90% $CD34^+$ cells, as determined by flow cytometry. $CD34^+$ cells were grown at a density of 10^5 cells/mL in α-MEM supplemented with 100 U/mL penicillin-streptomycin, 2 mmol/L L-glutamine, 10^{-6} mol/L hydrocortisone, 10^{-3} g/L nucleotide, 25×10^{-3} mg/L gentamicin, 10^{-4} mol/L 2-mercaptoethanol, 1% deionized BSA, 1 µg/mL cyclosporine A (all from Sigma-Aldrich), and 30% FBS (Gibco). The following recombinant cytokines were added to the media: 3 U/mL recombinant human (rH) erythropoietin (Janssen-Cilag), 20 ng/mL rH stem cell factor, and 10 ng/mL rH interleukin-3 (both PeproTech). Cell samples were collected at day 7, 9, and 14 of culture for cell counting and determination of cell viability. The erythroid cell antigen profile was analyzed using a cytofluorimetric strategy with the following surface markers: CD71 APC (anti-CD71 allophycocyanin–conjugated, clone M-A712), glycophorin A PE (phycoerythrin-conjugated anti-CD235a, clone GA-R2), and CD36 FITC (anti-CD36 fluorescein isothiocyanate conjugated, clone CB38) all from BD Biosciences (6). All the analyses were performed with the flow cytometer FACSCanto II (Becton Dickinson). The biparametric scatter plots were analyzed with FlowJo software version 7.6.4 (Becton Dickinson). Unstained cells were used as a negative control. Apoptosis was determined by double staining the cells with fluorescein isothiocyanate–conjugated Annexin-V and phycoerythrin (PE), using the human Annexin-V-PE Apoptosis Detection Kit (Bender MedSystems) according to the manufacturer's instructions.

References

1. Reagan-Shaw S, Nihal M, Ahmad N. Dose translation from animal to human studies revisited. *FASEB J.* 2008;22(3):659-61.
2. Matte A, et al. Peroxiredoxin-2 expression is increased in β-thalassemic mouse red cells but is displaced from the membrane as a marker of oxidative stress. *Free Radic Biol Med.* 2010;49(3):457–66.
3. Emma F, Montini G, Parikh SM, Salviati L. Mitochondrial dysfunction in inherited renal disease and acute kidney injury. *Nat Rev Nephrol.* 2016;12(5):267–80.
4. Palsson-McDermott EM, et al. Pyruvate kinase M2 regulates Hif-1alpha activity and IL-1beta induction and is a critical determinant of the warburg effect in LPS-activated macrophages. *Cell Metab.* 2015;21(1):65-80.
5. Matte A, et al. Peroxiredoxin-2: a novel regulator of iron homeostasis in ineffective erythropoiesis. *Antioxid Redox Signal.* 2018;28(1):1–14.
6. Beneduce E, et al. Fyn kinase is a novel modulator of erythropoietin signaling and stress erythropoiesis. *Am J Hematol.* 2019;94(1):10–20.
7. Matte A, et al. Bitopertin, a selective oral GLYT1 inhibitor, improves anemia in a mouse model of β-thalassemia. *JCI Insight.* 2019;4(22):e130111.

Supplemental Table 1. Effects of 3 weeks' treatment with mitapivat on hematological parameters and red cell indices in WT and Hbb$^{th3/+}$ mice

	WT mice, vehicle (*n* = 6)	WT mice, mitapivat (*n* = 6)	Hbb$^{th3/+}$ mice, vehicle (*n* = 14)	Hbb$^{th3/+}$ mice, mitapivat (*n* = 14)
Hematocrit, %	45.3 ± 0.55	46.1 ± 0.4	29.5 ± 1.6*	34.8 ± 0.8*°
CHCM, g/dL	26.7 ± 1.3	29.1 ± 0.4	24.5 ± 0.7	23.1 ± 0.5
MCH, pg	14.8 ± 0.2	14.4 ± 0.3	9.0 ± 0.3*	10.1 ± 0.3*°
MCVr, fL	55.2 ± 0.4	53.7 ± 1.2	51.2 ± 1.6*	55.0 ± 1.7°

CHCM, cell hemoglobin content mean; MCH, mean corpuscular hemoglobin; MCVr, reticulocyte mean corpuscular volume.

Data shown are mean ± SD.

*P < 0.05 compared with WT mice by 1-way ANOVA. °P < 0.05 compared with vehicle-treated Hbb$^{th3/+}$ mice by 1-way ANOVA.

Supplemental Table 2. Survival of CFSE-labeled red cells from WT (n = 4) and $Hbb^{th3/+}$ mice treated with vehicle or mitapivat (*n* = 3 each group).

	T_{50} (days)	T_{20} (days)
WT vehicle	18.9 ± 0.5	34.6 ± 1.0
$HBB^{th3/+}$ vehicle	9.6 ± 0.9 [A]	25.8 ± 0.8 [A,B]
$HBB^{th3/+}$ mitapivat	14.4 ± 0.4 [A]	31.1 ± 0.6 [A,B]

Data are mean ± SD. [A]*P* < 0.05 compared with WT and [B]*P* < 0.05 compared with vehicle by 1-way ANOVA with Dunnett's longitudinal comparison test.

Supplemental Table 3. List of primers used in quantitative real-time PCR

Gene	Forward primer sequence (5' → 3')	Reverse primer sequence (5' → 3')
Hamp	GCCTGAGCAGCACCACCTAT	TTCTTCCCCGTGCAAAGGCT
Cish	GGATCTGCTGTGCATAGCCAA	GCCTCGCTGGCTGTAATAGAAC
Serpin-3	CAAAGTCACATCCAGACAGAGCA	AGCTGAGTAGACAGGGCATCG
Id1	CACTGAGGGACCAGATGGACTC	GGTGGCTGCGGTAGTGTCTT
Erfe	ATGGGGCTGGAGAACAGC	TGGCATTGTCCAAGAAGACA
Dmt1-IRE	GCAGTGTTTGATTGCATTGG	TCTTCGCTCAGCAGGACTTT
Dmt1	TCTTCTGAACACCGTGGATG	CCGAAAGGGCTTAGAGAAAG
Atp6	CCACACACCAAAAGGACGAA	TGTGGTAAAAGGCCTAGGAGA
Yme1l	AACTACAGGACTTGATTCTGCGGT	GCTTCCTCCACCCCTTTAACAT
Pgc1a	GGAATGCACCGTAAATCTGC	GGCAAGAAACAGGAGATCGTTAAC
Mtco1	CTCCTAGCCGGAAATCTAGC	GGTTTCATGTTGATAATAGT
Cytb	GGCTTCTCAGTAGACAAAGCCA	TTGCTGGAGGAAGAGGAGGT
Ldha	TGGCTTGTGCCATCAGTATC	TCTCGCCCTTGAGTTTGTCT
Pkd1	AGCCTTCAGGAGTTGCTTGA	GTGCCGGTTTCTGATCCTTA
Pkm	GCTCGGCTGAATTTCTCTCA	GCAAAGCTTTCTGTGGCTTC
Pkm2	ACTACCCTCTGGAGGCTGTT	CGGAGTTCCTCGAATAGCTG
Slc2a1	CCCCAGAAGGTTATTGAGGA	AAAGCGTGGTGAGTGTGGTG
Pklr	CGCCTCAAGGAGATGATCAAG	CTCCGCATGGTACTCATGGGAG

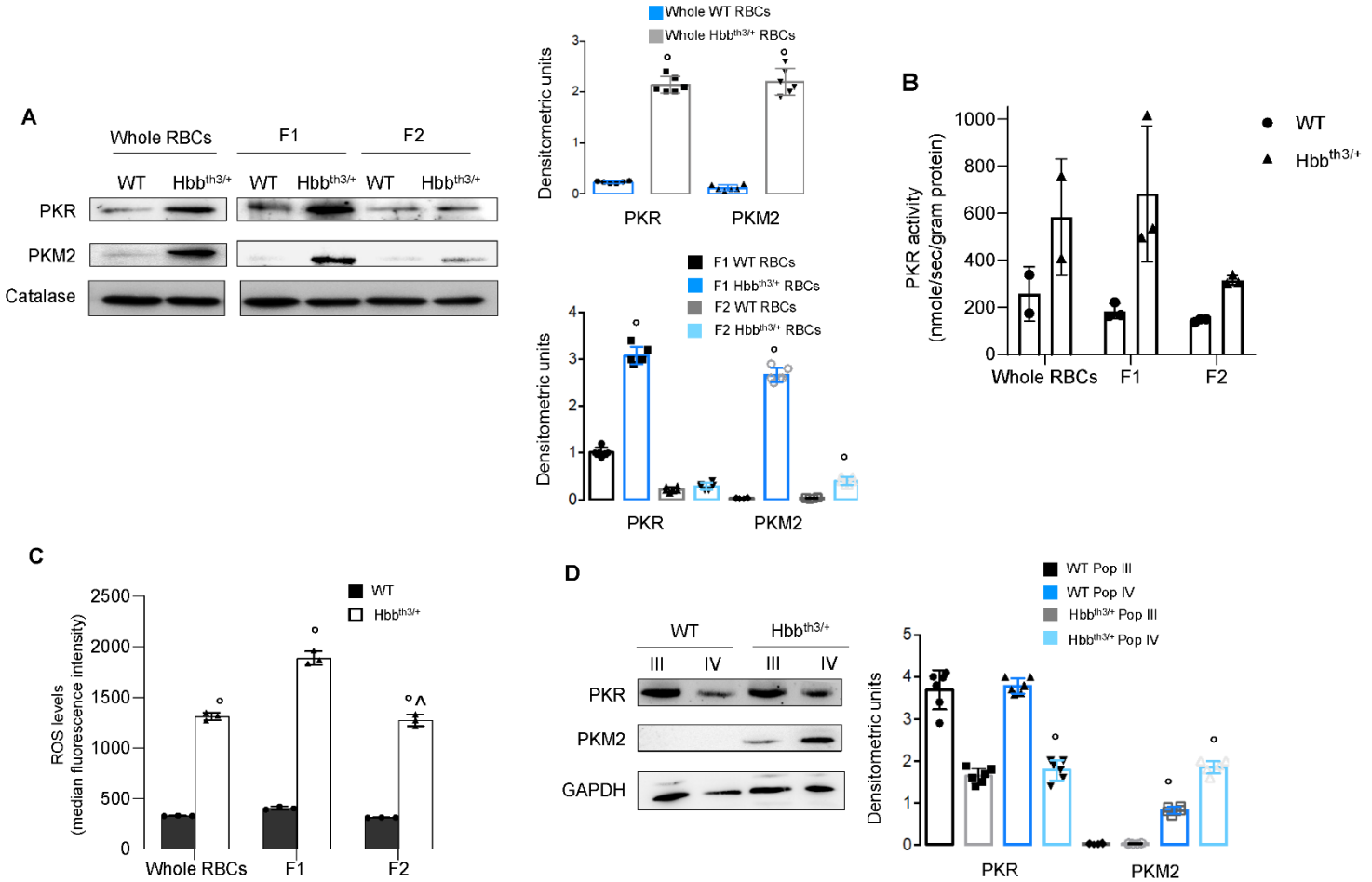

Supplemental Figure 1. The expression of pyruvate kinase isoforms is increased in both red cells and erythroid precursors from Hbb$^{th3/+}$ mice. (**A**, left panel) Western blot analysis of PKR and PKM2 in cytoplasm from whole red blood cells (RBCs) and from fractioned RBCs of WT or Hbb$^{th3/+}$ mice (n = 3). Catalase was used as a protein loading control. (**A**, right panels) Densitometric analyses of the western blot bands are shown in the left panel. Data are mean ± SD; n = 6. °P < 0.05 compared with WT by 2-way ANOVA with Tukey's multiple comparisons test. (**B**) PKR activity in whole (n = 2) or fractionated (n = 3) RBCs of WT and Hbb$^{th3/+}$ mice. Data are mean ± SD. (**C**) ROS levels in whole or fractionated RBCs of WT and Hbb$^{th3/+}$ mice (n = 3). Data are mean ± SD. °P < 0.05 compared with WT or ^P < 0.05 compared with reticulocyte-enriched red cell fraction (F1) by 2-way ANOVA with Bonferroni correction for multiple comparison. (**D**, left panel) Western blot analysis of PKR and PKM2 in polychromatic (pop III) and orthochromatic (pop IV) erythroblasts from WT Hbb$^{th3/+}$ mice (n = 3). GAPDH was used as a protein loading control. (**D**, right panel) Densitometric analyses of western blot bands are shown in the left panel. Data are mean ± SD (n = 6). °P < 0.05 compared with WT by 2-way ANOVA with Bonferroni correction for multiple comparison. F2, dense old red cells.

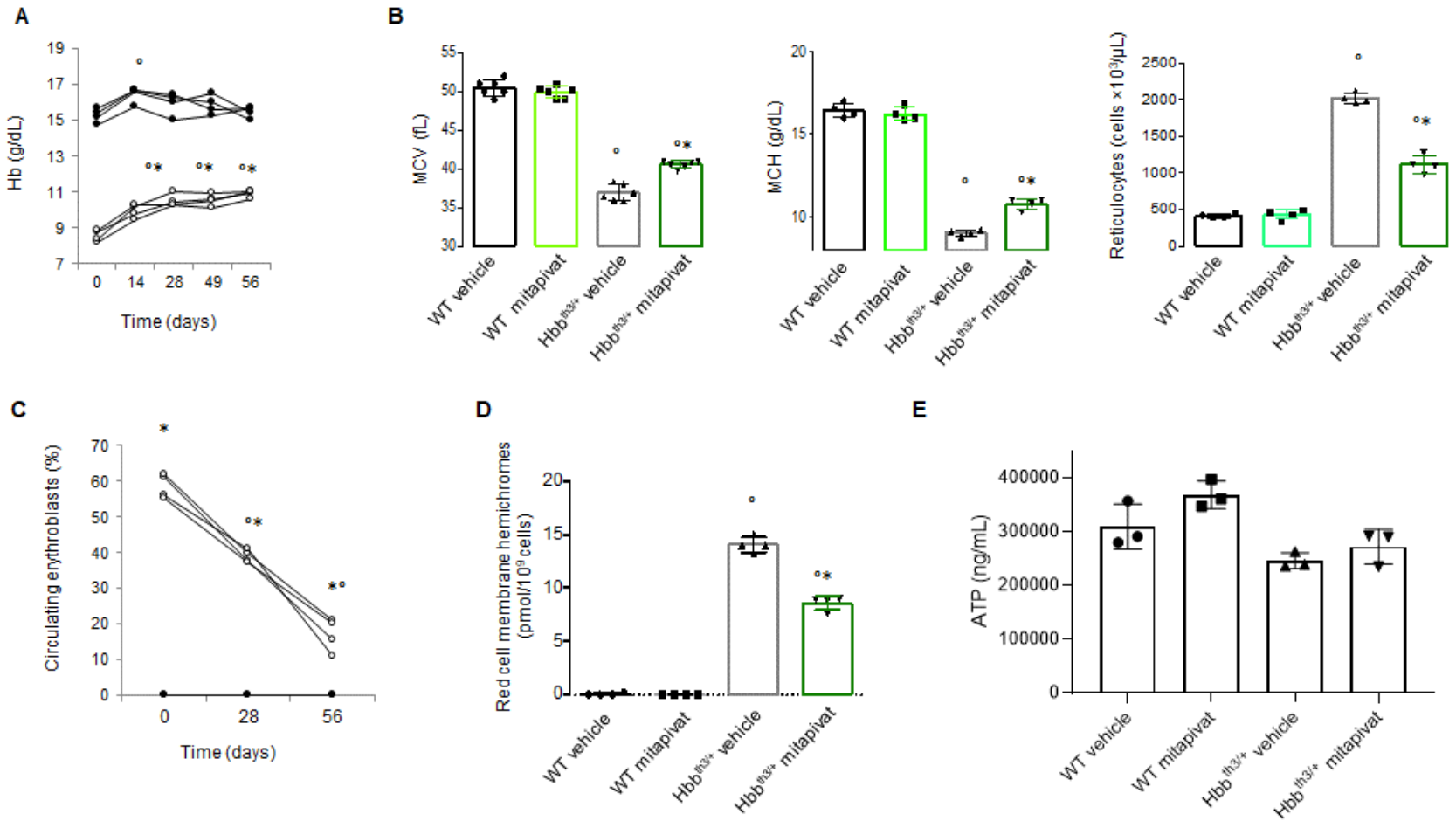

Supplemental Figure 2. In Hbb$^{th3/+}$ mice, long-term treatment with mitapivat beneficially affected hematologic parameters, and reduced circulating erythroblasts and red cell membrane–bound hemichromes. (**A**) Hemoglobin (Hb) in WT (n = 4; black circle) and Hbb$^{th3/+}$ (n = 4; empty circle) mice receiving long-term mitapivat treatment. Data are single mouse data. *P < 0.05 compared with WT mice or °P < 0.05 compared with baseline values by 1-way ANOVA with Dunnett's test for longitudinal comparison. (**B**) Mean corpuscular volume (MCV) (n = 6), mean corpuscular Hb (MCH) (n = 4), and reticulocyte count (n = 4) in WT and Hbb$^{th3/+}$ mice treated with vehicle or mitapivat for 56 days. Data are mean ± SD. °P < 0.05 compared with WT or *P < 0.05 compared with vehicle-treated Hbb$^{th3/+}$ mice by 1-way ANOVA with Bonferroni correction for multiple comparison. (**C**) Circulating erythroblasts in WT (black circle, n = 4) and Hbb$^{th3/+}$ (empty circle, n = 4) mice treated with mitapivat. *P < 0.05 compared with WT mice or °P < 0.05 compared with baseline values by 1-way ANOVA with Dunnett's test for longitudinal comparison. (**D**) Hemichromes bound to the red cell membrane from WT and Hbb$^{th3/+}$ (n = 4) mice treated with vehicle or mitapivat. Data are mean ± SD. °P < 0.05 compared with WT or *P < 0.05 compared with vehicle-treated animals by 1-way ANOVA with Bonferroni correction for multiple comparison. (**E**) ATP in whole blood of WT and Hbb$^{th3/+}$ mice treated with vehicle or mitapivat for 21 days. Data are mean ± SD, n = 3 per group.

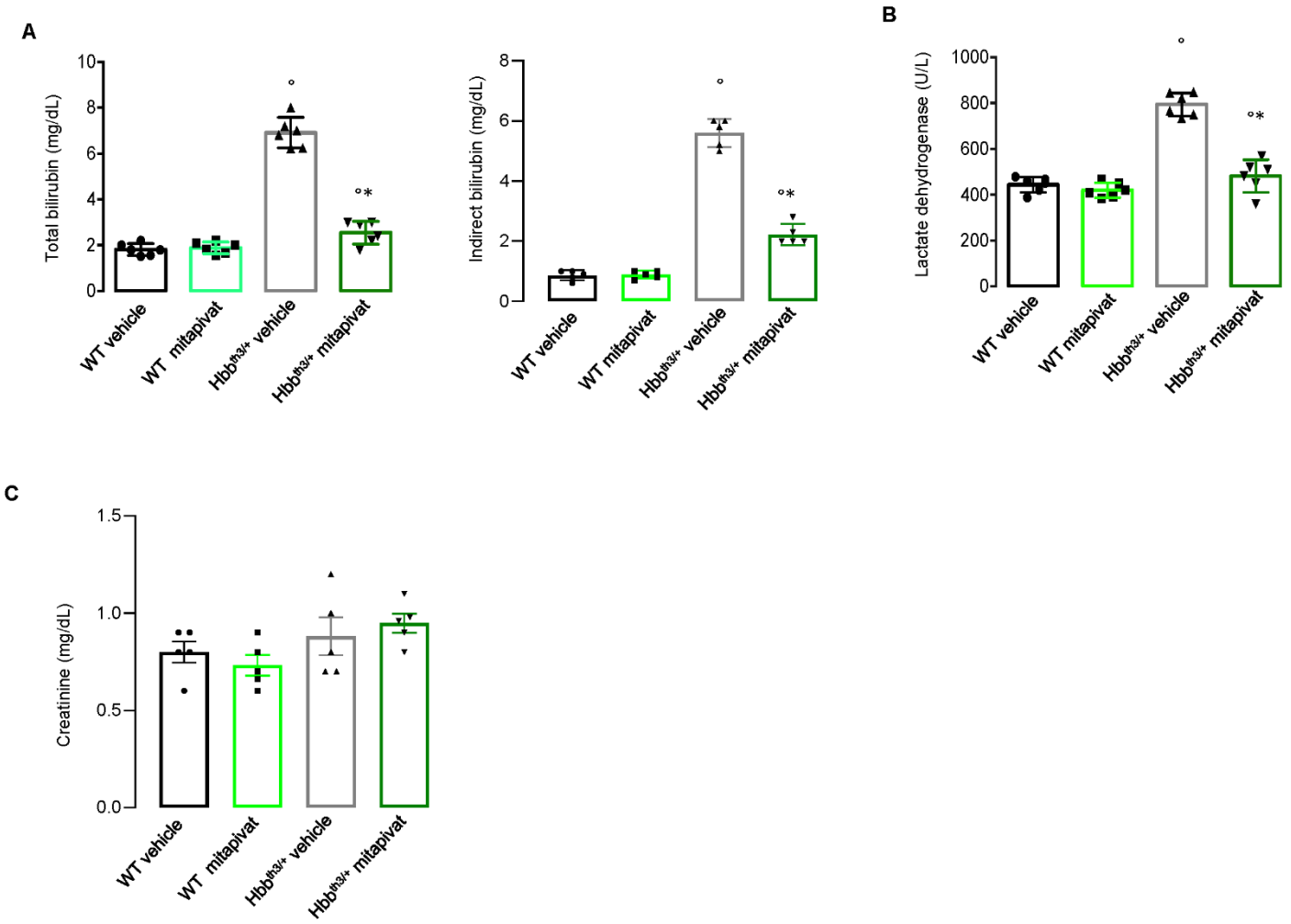

Supplemental Figure 3. Mitapivat treatment was associated with reduction in markers of hemolysis. (**A**–**B**) Plasma total bilirubin, indirect bilirubin and lactate dehydrogenase in WT and Hbb$^{th3/+}$ mice treated with vehicle or mitapivat. Data are mean ± SD, *n* = 6 per group. °*P* < 0.05 compared with WT or **P* < 0.05 compared with vehicle-treated animals by 1-way ANOVA with Bonferroni correction for multiple comparison. (**C**) Plasma creatinine in WT and Hbb$^{th3/+}$ mice treated with vehicle or mitapivat. Data are mean ± SEM, *n* = 5 per group.

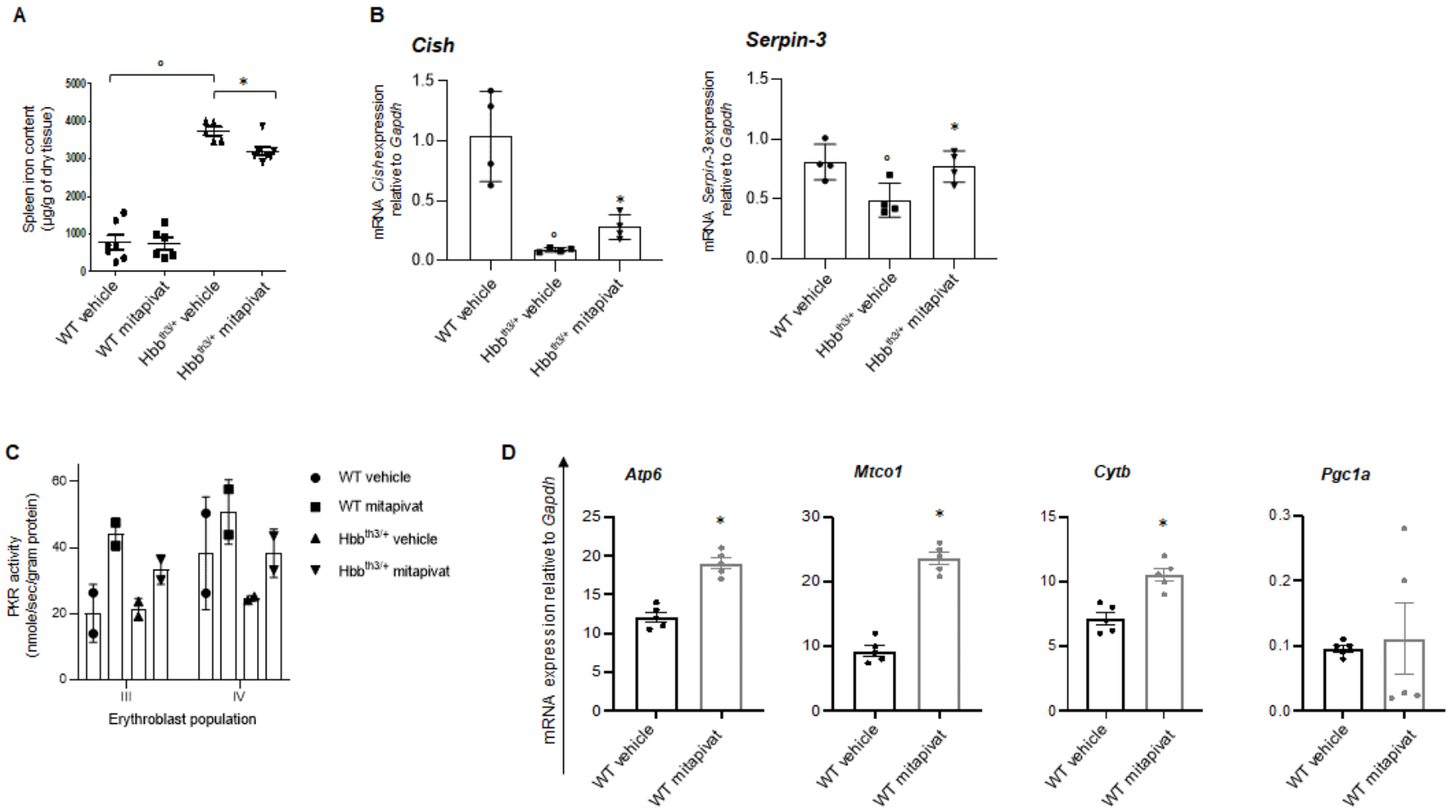

Supplemental Figure 4. Mitapivat ameliorated spleen iron content and improved erythropoietin responsiveness in sorted erythroblasts from Hbb$^{th3/+}$ mice. (**A**) Spleen non-heme iron content in WT (n = 6–7) and Hbb$^{th3/+}$ (n = 5–7) mice treated with vehicle or mitapivat. Data are mean ± SD. (**B**) mRNA expression of *Cish* and *Serpin-3* by quantitative real-time PCR of sorted erythroblasts from bone marrow of WT and Hbb$^{th3/+}$ mice treated with vehicle or mitapivat. Data are mean ± SD (n = 4). (**C**) PKR activity in erythroblasts from vehicle Hbb$^{th3/+}$ mice versus mitapivat treated Hbb$^{th3/+}$ mice. Data are mean ± SD (n = 2 per group). (**A**–**B**) °P < 0.05 compared with WT or *P < 0.05 compared with vehicle-treated animals by 2-way ANOVA with Bonferroni correction for multiple comparison. (**D**) mRNA expression of *Atp6*, *Mtco1*, *Cytb*, and *Pgc1a* genes by quantitative real-time PCR on sorted erythroblasts from bone marrow of WT mice treated with vehicle or mitapivat. Data are mean ± SD (n = 5 per group). *P < 0.05 compared with vehicle-treated mice by 2-way ANOVA with Bonferroni multiple comparison correction.

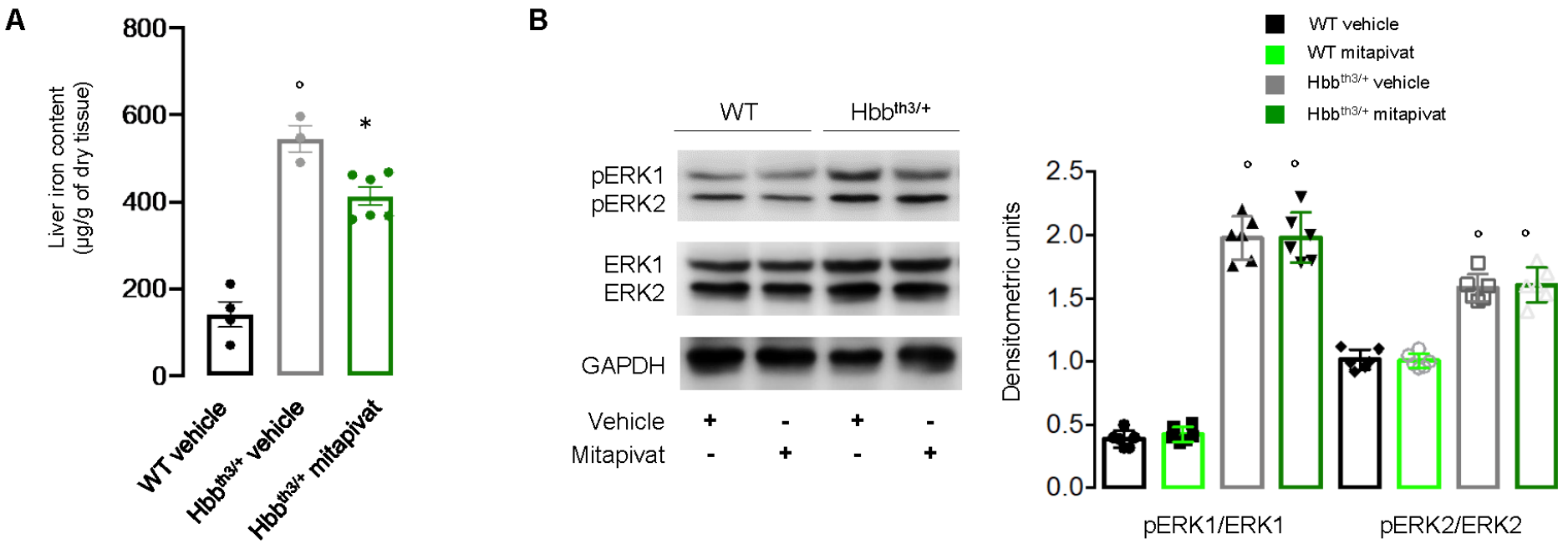

Supplemental Figure 5. Mitapivat significantly reduces liver non-heme iron content in Hbb$^{th3/+}$ mice. (**A**) Liver non-heme iron content in WT (n = 4) and Hbb$^{th3/+}$ (n = 3–6) mice treated with vehicle or mitapivat. Data are mean ± SEM. °P < 0.05 compared with WT; *P < 0.05 compared with vehicle treated animals by 1-way ANOVA with Bonferroni correction for multiple comparison**.** (**B**) Western blot analysis of pERK1/2 and ERK1/2 in livers from WT and Hbb$^{th3/+}$ mice treated with vehicle or mitapivat. One representative of 4 independent experiments is shown. Right panel, densitometric analyses of western blot bands. Data are mean ± SD (n = 6). °P < 0.05 compared with WT by 1-way ANOVA with Bonferroni correction for multiple comparison.

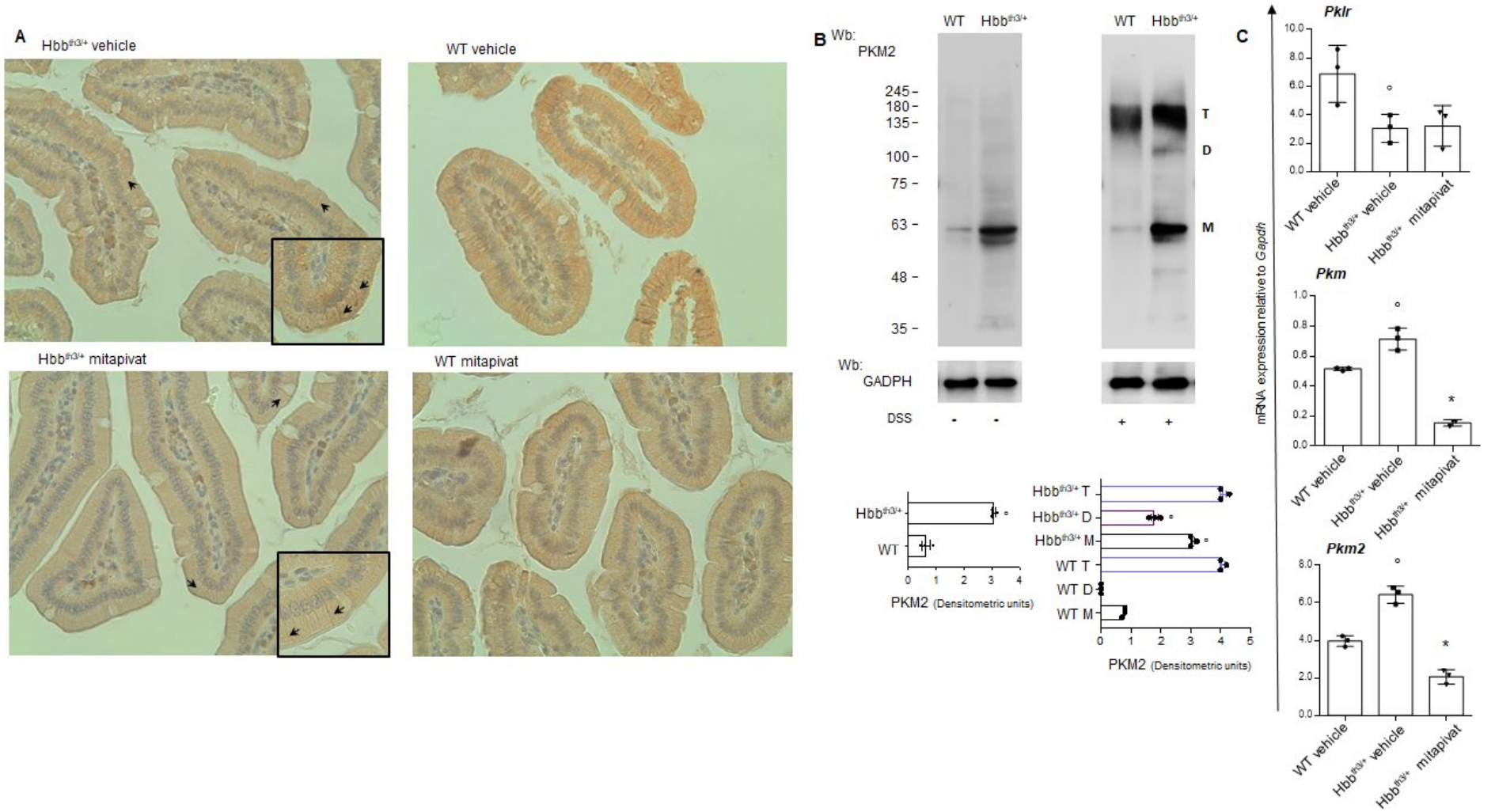

Supplemental Figure 6. Mitapivat treatment reduced duodenum PKM2 expression in Hbb$^{th3/+}$ mice. (**A**) Representative immunohistochemical analysis of ferroportin (FPN1) in duodenums of Hbb$^{th3/+}$ (left panels) or WT (right panels) mice with or without mitapivat treatment. Arrows indicate the basolateral membrane localization of FPN1. Magnification 40×. (**B**) Immunoblot analysis of PKM2 expression in duodenum from WT and Hbb$^{th3/+}$ mice with and without disuccinimidyl suberate cross-linking. One representative image of 3 overall with similar results. T: tetramers; D: dimers; M: monomers. Data are mean ± SEM (n = 3). °P < 0.05 compared with WT by 1-way ANOVA with Bonferroni correction for multiple comparison. (**C**) mRNA expression of *Pklr* and *Pkm2* by quantitative real-time PCR on duodenums of WT and Hbb$^{th3/+}$ mice with and without mitapivat. Data are mean ± SD, n = 6 per group. °P < 0.05 compared with WT or *P < 0.05 compared with vehicle-treated animals by 2-way ANOVA with Bonferroni correction for multiple comparison.

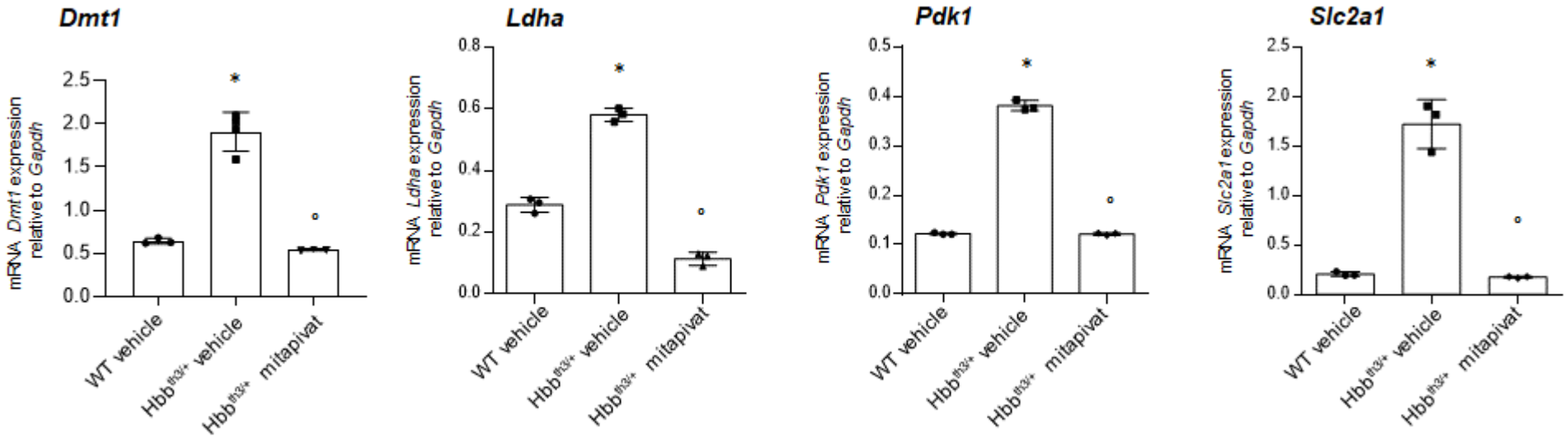

Supplemental Figure 7. Mitapivat reduced PKM2-HIF target genes in duodenum of Hbb$^{th3/+}$ mice. mRNA expression of *Dmt1* (non-IRE), *Ldha, Pdk1, Slc2a1* by quantitative real-time PCR on duodenums from WT (n = 3) and Hbb$^{th3/+}$ mice treated with vehicle (n = 4) or mitapivat (n = 3). Data are mean ± SD. *P < 0.02 compared with WT mice or °P < 0.05 compared with vehicle-treated mice by 2-way ANOVA with Tukey's multiple comparisons test.

Supplemental Figure 8

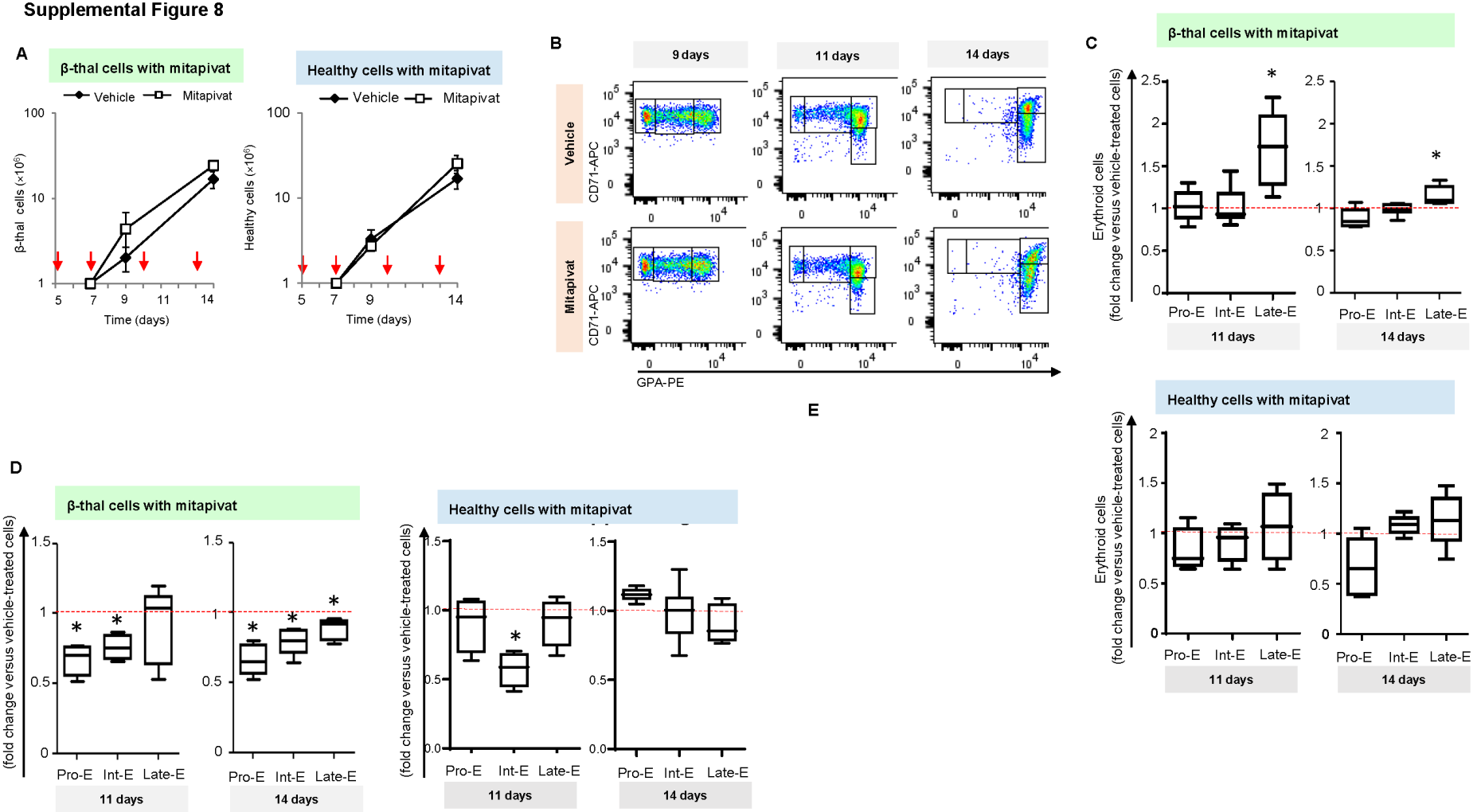

Supplemental Figure 8. Mitapivat beneficially affected in vitro β-thalassemic erythropoiesis. (**A,** left panel)**.** Proliferation of β-thalassemic erythroid precursors treated with vehicle or mitapivat in in vitro liquid culture of CD34+ cells isolated from peripheral blood of patients with β-thalassemia (*n* = 3). Red arrows indicate when mitapivat was added to the culture medium. Data are mean ± SD. (**A**, right panel)**.** Cell proliferation of healthy erythroid precursors treated with vehicle (*n* = 8) or mitapivat (*n* = 3) in in vitro liquid culture of CD34⁺ cells isolated from peripheral blood of healthy subjects. Red arrows indicate when mitapivat was added to the culture medium. Data are mean ± SD. (**B**) Effect of mitapivat on maturation pattern of β-thalassemic erythroid precursors from a single patient at 9, 11, and 14 days of culture with vehicle or mitapivat. Representative flow cytometric plots showing the differentiation pattern of β-thalassemic erythroid precursors. CD36, glycophorin-A (GPA), and CD71 were used as surface markers to identify the following homogenous cell populations:

erythroid colony-forming unit, pro-erythroblasts (Pro-E), basophilic erythroblasts corresponding to intermediate erythroblasts (Int-E), and polychromatic and orthochromatic erythroblasts as late erythroblasts (Late-E). (**C,** upper panel). Effect of mitapivat on maturation pattern of β-thalassemic erythroid precursors from a single patient at 9, 11, and 14 days of culture with vehicle or mitapivat. Representative flow cytometric plots showing the differentiation pattern of β-thalassemic erythroid precursors. CD36, glycophorin-A (GPA), and CD71 were used as surface markers to identify the following homogenous cell populations: erythroid colony-forming unit, pro-erythroblasts (Pro-E), basophilic erythroblasts corresponding to intermediate erythroblasts (Int-E), and polychromatic and orthochromatic erythroblasts as late erythroblasts (Late-E). (**C**, lower panel). Effect of mitapivat on the index of erythroid maturation of healthy cells from 4 separate individuals at 11 (n = 4) and 14 (n = 10) days of cell culture. CD36, glycophorin-A, and CD71 were used as surface markers, in order to identify the following homogenous cell populations: erythroid cell forming units, pro-erythroblasts (Pro-E), basophilic erythroblasts corresponding to intermediate erythroblasts (Int-E), and polychromatic and orthochromatic erythroblasts as late erythroblasts (Late-E). (**D,** left panel)**.** Effect of mitapivat on the amount of annexin-V+ cells during β-thalassemic erythroid maturation from 4 separate individuals at 11 and 14 days of cell culture (n = 5). (**D**, right panel)**.** Effect of mitapivat on the amount of annexin-V+ cells during erythroid maturation from 4 separate healthy individuals at 11 (n = 4) and 14 (n = 6) days of cell culture. (**C** and **D**) Data are shown as median and minimum/maximum, with boxes indicating 25th–75th percentiles; *P < 0.05 compared with vehicle-treated cells by 2-tailed unpaired Student t test with Bonferroni correction for multiple comparisons.